Start Current and Gain Measurements for a Smith-Purcell Free-Electron Laser

J. Gardelle and P. Modin
CEA, CESTA, F-33114 Le Barp, France

J. T. Donohue
Centre d'Etudes Nucléaires de Bordeaux-Gradignan, Université Bordeaux 1, CNRS/IN2P3, BP 120, 33175 Gradignan, France
(Received 19 July 2010; published 23 November 2010)

Coherent Smith-Purcell radiation is a promising source of coherent emission in the THz domain. Although it has been observed in several experiments, some physical quantities related to the bunching of an initially continuous beam had not yet been studied experimentally. Among them, the gain as function of beam current, together with the value of the start current, needed to be addressed. We report here their measurements in a microwave experiment using a sheet beam. A start current of about 20 A/m was found. Two-dimensional simulations with a very thin beam agree well with our results.

DOI: 10.1103/PhysRevLett.105.224801 PACS numbers: 41.60.Cr, 52.65.Rr

If an electron beam passes near a diffraction grating, it produces radiation. When, in 1953, Smith and Purcell (SP) [1] sent a 300 keV electron beam along a grating of period 1.67 μm, they observed incoherent visible light that satisfied the condition $\lambda = L(1/\beta - \cos\theta)/|n|$, where λ denotes the wavelength of radiation produced at angle θ with respect to the beam, L is the period, n is the order of diffraction, and $\beta = v/c$ is the usual relative velocity. Since its discovery, SP radiation has been the subject of much theoretical and experimental work. The use of coherent SP radiation as a diagnostic tool for measurements of bunch length has been demonstrated over a wide range of beam energies [2–4]. Recently there has been renewed interest in coherent Smith-Purcell (CSP) free-electron devices that may be used as compact, tunable sources for coherent THz radiation. Much of this was inspired by the work of Andrews and Brau (AB) [5], who established the dispersion relation between frequency ω and axial wave number k for the evanescent wave on a lamellar grating. Their analysis was two-dimensional (2D), i.e., no dependence in the direction along the grooves. Assuming the beam to be uniform plasma moving above the grating, they calculated the gain of the beam-wave interaction, finding a result similar to that found by Pierce for traveling wave tubes [6]. In particular, they predicted that the gain would be proportional to $I^{1/3}$, where I is the current. However, they also pointed out two features which earlier analyses had overlooked. At sufficiently low beam energy, the intersection of the beam line, $\omega = vk$, occurs on the downward sloping portion of the dispersion relation, as in a backward wave oscillator. This allows for feedback even without reflection from the grating ends. Secondly, they noted that the evanescent wave's frequency is always less than the minimum allowed SP frequency. The evanescent wave then emits omnidirectional radiation upon reaching the ends of the grating. If, however, the bunching at that frequency is strong, higher harmonics will appear in the current, and these may correspond to allowed SP frequencies. When this happens, what Andrews *et al.* call superradiance occurs [7], where the emissions from successive bunches interfere so as to produce coherent radiation only at harmonics of the bunching frequency. For each harmonic the radiation satisfies the SP relation between angle and frequency, and thus is emitted only in a small angular range.

This theory was supported by simulations using particle-in-cell (PIC) codes [8,9], in this case with the commercial code MAGIC [10]. Kumar and Kim (KK) [11] considered a sheet electron beam of zero thickness moving above the grating, rather than a uniform plasma, but still found results not unlike those of AB. They estimated the threshold or start current needed to overcome losses and produce gain. A significant difference between AB and KK is that the former relate gain to the current density of the moving plasma (A/m^2) while the latter relate gain to the linear current density of their infinitesimally thick beam (A/m). Mkrtchian [12] has given a general discussion of gain that considers a beam of arbitrary thickness, thus providing a bridge between the models of AB and of KK. He also discusses the effect of a uniform magnetic guide field on gain, which is that a beam in a magnetic field requires twice as much current for the same gain. Except for the results found by Skrynnik and co-workers [13] at extremely low energy, 2–5 keV, no observations of SP radiation with continuous beams agreed with theory. However, two recent experiments have confirmed certain aspects of it. The first [14], which used a narrow round beam, observed the evanescent wave at the expected sub-SP frequency. The second [15], using an intense (200 A), wide (10 cm) and thin (5 mm) beam, was able to observe not only the evanescent wave (4.6 GHz) but also its second (9.2 GHz) and third (13.8 GHz) harmonics. The beam bunching was observed directly with a current monitor and also with a magnetic probe placed at the end of a

 © 2010 The American Physical Society

groove. The results conformed to the scenario outlined by AB. They were also consistent with the 2D MAGIC simulations presented in Ref. [8].

Here we report on a new experiment that addresses a critical issue, the dependence of gain on current. By varying the beam current we have found the threshold value needed to produce bunching with exponential growth in time. The experimental configuration has been described in Ref. [15]. The grating dimensions were those of the simulations reported in Ref. [8], except that the grating width was 10 cm. The parameters are summarized in Table I. In order to have a system in which the 2D approximation may be valid, we used a wide sheet beam (10 cm), produced by a thin copper cathode. In our previous experiment, we were unable to vary significantly the beam current. However, in the new one, we added a slit at the grating entrance, which is visible in Fig. 1(a). With this, the current of the electron beam can be varied from 0 to the maximum value (280 A) by changing the slit thickness. The generator driving the diode operates in single-shot mode. Both diode and grating are enclosed in a cylindrical vacuum chamber, which is surrounded by a pulsed solenoid that provides a uniform axial magnetic field. As may be seen in Fig. 1(a), a B-dot probe is placed at the end of a groove in the grating. This is used to measure B_x, the magnetic field component of the evanescent mode.

In Fig. 1(b), we show the MAGIC 2D geometry used to simulate this experiment. The mesh size is 100 μm in the vicinity of the beam. In one series of simulations we have used fits to the experimental voltage and current curves as input conditions in MAGIC, while in two other series a 1-ns rise time to the nominal value was used. In one of these a beam of zero thickness was emitted, as in KK, while in the other a uniform beam of vertical height 2 cm was employed, to simulate AB.

The voltage applied to the diode is measured with a capacitive sensor, while the current is measured by a Rogowski coil downstream from the grating on the current return stalk. Typical $V(t)$ and preslit $I(t)$ waveforms from the same oscilloscope are displayed in Fig. 2(a). The maximum current (slit wide open) is 280 A at 95 kV, for

TABLE I. Experimental parameters.

Parameters	Value
Beam kinetic energy	95 keV
Peak current	0–280 A
Pulse duration	300 ns
Beam thickness ε	0.01–2 mm
Beam-grating distance	3 mm
Grating period L	2 cm
Groove depth H	1 cm
Groove width A	1 cm
Grating width	10 cm
Number of periods	20
External magnetic field	0.3–0.5 T

a pulse of duration 300 ns (FWHM). Figure 2(b) shows the collected current after passage above the grating when the slit thickness is 100 μm. The low-pass filtered current I_0 (blue curve) is 7 A. Because the voltage varies slightly during the interaction, we expect to observe a variation of the bunching frequency by performing a sliding fast-Fourier-transform (FFT) algorithm. This measurement turns out to give the actual beam kinetic energy (red curve), because the CSP interaction occurs at the intersection between the beam line (slope β) and the grating dispersion relation $\omega(k)$. This time variation is small, and the FFT spectra of both the collected current and the B-dot probe signals peak strongly near 4.6 GHz. They are shown in Fig. 2(c), and the former has been normalized arbitrarily so that the peak values of both curves coincide.

The exponential growth rate of the interaction, Im(ω), is obtained by measuring the slope of the envelope of the rf part of the B-dot signal in a log-scale plot. This is indicated in Fig. 2(d), for the shot whose current was shown in Fig. 2(b). Both are from the same oscilloscope, which is not that used for Fig. 2(a). The measured signal (green curve) is the time derivative of the B_x component of the grating mode, after filtering around the nominal 4.6 GHz frequency. At early time, one sees noise, from which then emerges an exponentially growing signal. Finally, saturation is reached at a level 2 orders of magnitude above noise. The noise level and dynamic range of our oscilloscope limited our observations to gains of this order, regardless of current. For comparison, the results of a 2D MAGIC simulation (red curve) of B_x in the groove are shown. The simulation predicts a growth rate about twice that of the experiment, which we consider acceptable agreement. We note that the analysis of the rf signal of the evanescent wave, detected by a horn in the far field region, gives a similar growth rate. The evanescent wave is

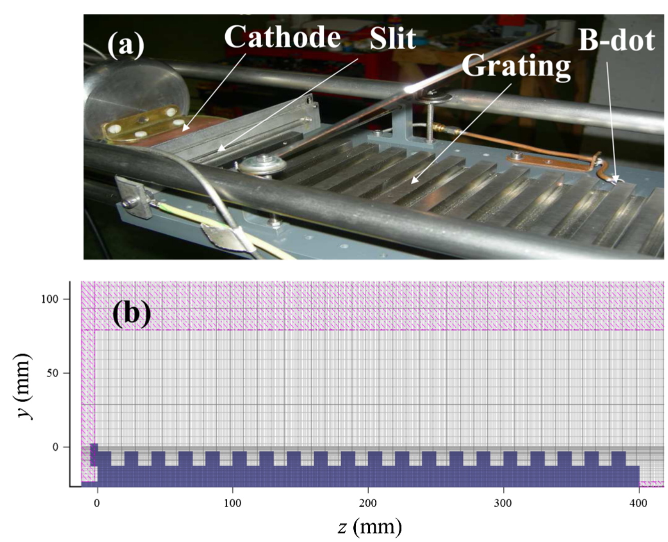

FIG. 1 (color online). (a) Photograph of the setup. A slit is placed between the cathode and the grating to vary the beam current. (b) MAGIC 2D geometry used to simulate the experiment.

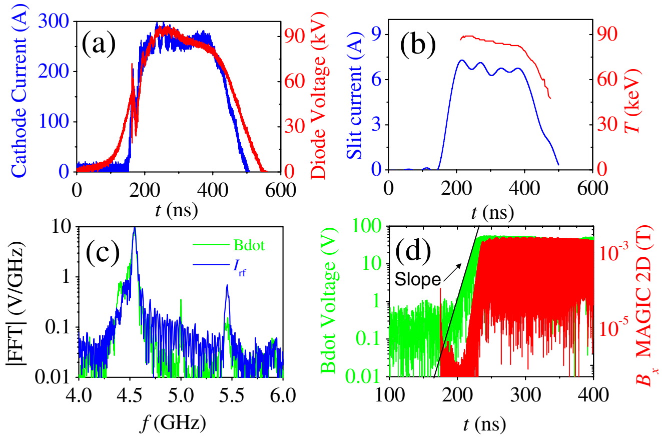

FIG. 2 (color online). Time signals and their FFTs. (a) Diode voltage (red curve) and cathode current (blue curve) versus t. (b) Collected current (blue curve), and beam kinetic energy (red curve) as deduced from a sliding FFT of the rf current, versus t. (c) FFT spectra of the B-dot signal (green lines) and collected current I_{rf} (blue lines, arbitrary units). (d) Log-scale plots of the B-dot signal (green lines) and simulated B_x (red lines) versus t.

emitted from the ends of the grating, and some of it emerges from the vacuum chamber through a plastic window. Our analysis of gain versus current uses only the B-dot probe signals.

The main result is given in Fig. 3. Slit thickness was varied by moving the upper lip, the other remaining at 3 mm from the grating surface. The analysis is complicated by the fact that for current values $I_0 > 10$ A, the exponential growth starts during the rise time (50 ns) of the current pulse. Consequently, in Fig. 3(a), we have plotted the gain, not as a function of I_0, but rather as a function of I_1, the current at the time t_1 when oscillation starts. Each point represents average values of $\mathrm{Im}(\omega)$ and I_1 for five identical shots, and the corresponding statistical (1σ) error bars are shown. We show two fits to these data. The red curve assumes that the data may be fitted with a simple three-parameter expression, $\mathrm{Im}\omega = \alpha\theta(I_1 - I_{\mathrm{th}})(I_1 - I_{\mathrm{th}})^{\nu}$, where θ denotes the Heaviside step function, I_{th} the threshold current in amperes, and ν and α are free parameters. We find for the best fit (reduced $\chi^2 = 1.23$): $\alpha = (0.119 \pm 0.011) \times 10^9\ \mathrm{s}^{-1}$, $I_{\mathrm{th}} = (2.48 \pm 0.09)$ A, $\nu = 0.53 \pm 0.05$. This being an empirical formula, we attach no deep significance to α and ν, but we note that the threshold or start current is of the order of 2 A. The blue curve is similar, except that ν is fixed at $1/3$, the same I_{th} is imposed, and we find $\alpha = 0.25 \pm 0.09$. The fit with the imposed exponent of $1/3$ is better at higher currents, but not as good at lower values. In principle, it should be easy to distinguish between these choices, but in practice, we cannot greatly increase the current I_1, since the gain starts long before I_0 is reached. Despite the increasing current in a shot, we do not observe any noticeable curvature in the logarithm of the signal, at least over the range we observe.

We have also performed 2D simulations for 23 values of beam current; the results are shown in Fig. 3(b). In 2D

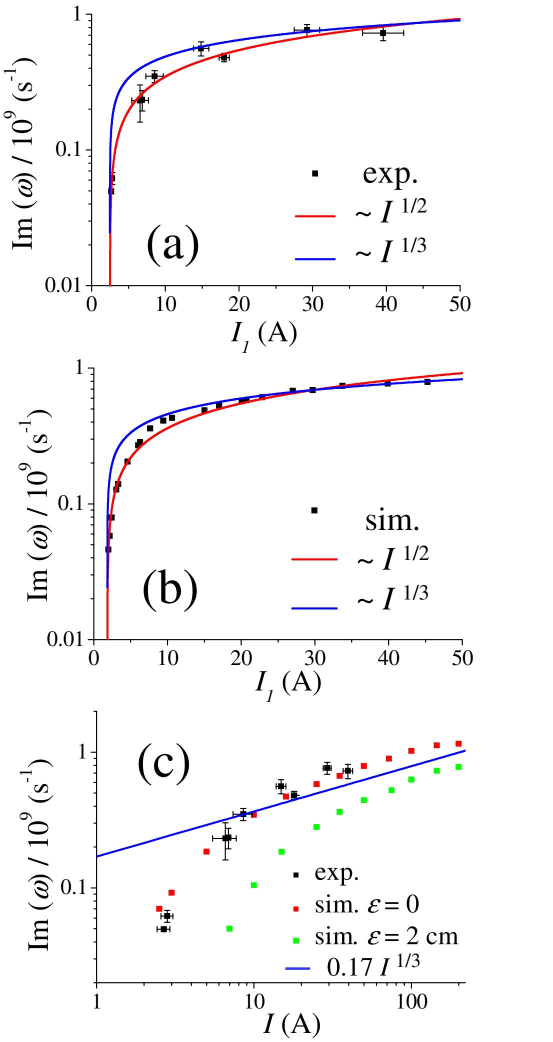

FIG. 3 (color online). Gain curve and start current: $\mathrm{Im}\omega$ vs I_1. (a) Experiment (black squares), empirical three-parameter fit (red curve), asymptotic $I_1^{1/3}$ fit (blue curve). (b) 2D MAGIC predictions: (black squares) along with three-parameter fit (red curve) and asymptotic $I_1^{1/3}$ fit (blue curve). (c) Data (black squares), and 2D simulations with 1 ns rise time, red squares $\varepsilon = 0$, green squares $\varepsilon = 2$ cm. For comparison, a simple power law $0.17\ I_1^{1/3}$ is shown by the blue line.

simulations, the relevant current is really a linear current density, whose dimension is A/m. Given our grating width of 10 cm, the true linear current density is 10 I_1. These simulations were performed with beam thickness of 100 μm, and we checked that the gain remained unchanged provided the slit thickness did not exceed 2 mm. We have taken into account the error we make when estimating the slope of the MAGIC result presented in Fig. 2(d). The red curve is a fit of these MAGIC predictions with the same function we used to fit the experimental data. We find: $\alpha = (0.119 \pm 0.011) \times 10^9\ \mathrm{s}^{-1}$, $I_{\mathrm{th}} = (1.84 \pm 0.01)$ A, $\nu = 0.53 \pm 0.01$. The blue curve is again with $\nu = 1/3$, this value of I_{th}, and we find $\alpha = 0.23 \pm 0.02$. Compared to the experimental fit, the main difference

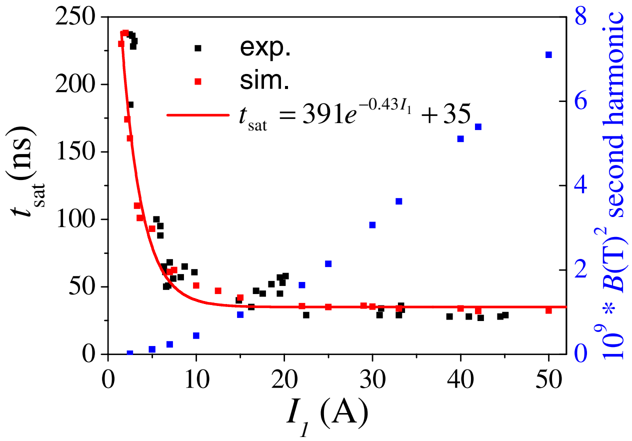

FIG. 4 (color online). Left-hand scale: Time needed to reach saturation, t_{sat} versus current I_1, experiment (black squares), 2D MAGIC predictions (red squares), along with empirical fit. Right-hand scale, simulated B_x^2 at saturation vs I_1, filtered at second harmonic (blue squares).

is a smaller value of the threshold current, I_{th}. The agreement between Figs. 3(a) and 3(b) is reasonable. In both curves, the start current is approximately 2 A, the asymptotic behaviors are similar ($I_1^{1/3}$), but, if we fit the whole range of current, our best fit is with $I_1^{0.5}$.

In order to avoid the problem of gain occurring on the rising current, and thereby obtain currents greater than those accessible to our experiment, we have also performed simulations with 1 ns rise times. The motivation is twofold: to reach higher currents and to compare the effects of a zero thickness beam with those of a thick (2 cm) beam. For our energy, the evanescent wave decreases with an e-folding distance of 0.68 cm above the grating. The results are shown in Fig. 3(c) in a log-log plot. The experimental results are shown again, together with the simulations with thickness $\varepsilon = 0$ (red squares) and $\varepsilon = 2$ cm (green squares). A simple 1/3 power law is also indicated, to show that both simulations are consistent with it at high linear current densities (> 400 A/m). Clearly the zero thickness simulation is in good agreement with our data. The $\varepsilon = 2$ cm simulation requires more current to produce a given gain, and seriously overestimates the start current. We see in the simulations that only that part of the current within a centimeter of the grating is bunched.

Another interesting result is illustrated in Fig. 4, where the saturation time is plotted as a function of I_1. The black squares are the experimental points, the red squares are 2D MAGIC predictions along with a three-parameter exponential decay fit (red curve): $t_{sat} = 391e^{-0.43I_1} + 35$. For high currents, $I_1 > 10$ A, saturation of the interaction is fast and occurs during the 50 ns rise time. For smaller currents, $I_1 < 3$ A, bunching and gain occur after the current has reached its maximum value, but the pulse drops off before saturation is reached. On the right-hand scale of this figure, we show as blue squares the simulated value at saturation of B_x^2, filtered at the second harmonic (9.2 GHz), and observed at a point situated approximately 6 cm above the middle of the grating. This quantity is proportional to the power radiated at the second harmonic, and it is seen to exhibit a quadratic dependence on current. If this were to be confirmed experimentally (our oscilloscope bandwidth was too small for us to see this) it would indicate substantial energy flux (100 W/cm^2 at 50 A).

We conclude there is reasonable agreement between our experimental results and both 2D theory and simulations. In particular, simulations with a zero thickness beam, as recommended by KK, agree quite well with our measurements of gain and start current. We conclude that provided experimental conditions permit, the use of a wide ultrathin beam should be preferred to a thicker beam. Furthermore, results of 2D simulations can be used as a reliable guide for choosing the experimental parameters in future experiments. In this way, the goal of attaining compact Smith-Purcell THz sources may be attained.

[1] S. J. Smith and E. M. Purcell, Phys. Rev. **92**, 1069 (1953).
[2] A. S. Kesar, R. A. Marsh, and R. J. Temkin, Phys. Rev. ST Accel. Beams **9**, 022801 (2006).
[3] G. Doucas *et al.*, Phys. Rev. ST Accel. Beams **5**, 072802 (2002).
[4] V. Blackmore *et al.*, Nucl. Instrum. Methods Phys. Res., Sect. B **266**, 3803 (2008).
[5] H. L. Andrews and C. A. Brau, Phys. Rev. ST Accel. Beams **7**, 070701 (2004).
[6] J. Pierce, *Traveling-Wave Tubes* (Van Nostrand, New York, 1950).
[7] H. L. Andrews *et al.*, Phys. Rev. ST Accel. Beams **8**, 110702 (2005).
[8] J. T. Donohue and J. Gardelle, Phys. Rev. ST Accel. Beams **8**, 060702 (2005).
[9] D. Li *et al.*, Phys. Rev. ST Accel. Beams **9**, 040701 (2006).
[10] B. Goplen *et al.*, Comput. Phys. Commun. **87**, 54 (1995).
[11] Vinit Kumar and Kwang-Je Kim, Phys. Rev. E **73**, 026501 (2006).
[12] G. F. Mkrtchian, Phys. Rev. ST Accel. Beams **10**, 080701 (2007).
[13] B. K. Skrynnik, V. K. Korneyenkov and M. Yu. Demchenko, Telecommun. Radio Eng. **55**, 170 (2001).
[14] H. L. Andrews *et al.*, Phys. Rev. ST Accel. Beams **12**, 080703 (2009).
[15] J. Gardelle *et al.*, Phys. Rev. ST Accel. Beams **12**, 110701 (2009).